

UCLA

UCLA Previously Published Works

Title

Expression and Therapeutic Potential of SOX9 in Chordoma

Permalink

<https://escholarship.org/uc/item/43g5v7s3>

Journal

Clinical Cancer Research, 23(17)

ISSN

1078-0432

Authors

Chen, Hua
Garbutt, Cassandra C
Spentzos, Dimitrios
et al.

Publication Date

2017-09-01

DOI

10.1158/1078-0432.ccr-17-0177

Peer reviewed



Published in final edited form as:

Clin Cancer Res. 2017 September 01; 23(17): 5176–5186. doi:10.1158/1078-0432.CCR-17-0177.

Expression and Therapeutic Potential of SOX9 in Chordoma

Hua Chen^{1,2}, Cassandra C. Garbutt¹, Dimitrios Spentzos¹, Edwin Choy¹, Francis J. Hornicek¹, and Zhenfeng Duan¹

¹Sarcoma Biology Laboratory, Department of Orthopaedic Surgery, Massachusetts General Hospital and Harvard Medical School, 55 Fruit Street, Jackson 1115, Boston, Massachusetts 02114

²Department of Emergency Surgery, ShenZhen People's Hospital, 2nd Clinical Medical College of Jinan University, No.1017 Dongmenbei Road, Shenzhen, Guangdong Province, China, 518020

Abstract

Purpose—Conventional chemotherapeutic agents are ineffective in the treatment of chordoma. We investigated the functional roles and therapeutic relevance of the sex-determining region Y (SRY)-box 9 (SOX9) in chordoma.

Experimental Design—SOX9 expression was examined by immunohistochemistry (IHC) using 50 chordoma tissue samples. SOX9 expression in chordoma cell lines was examined by Western blot and immunofluorescence assays. We used synthetic human SOX9 siRNA to inhibit the expression of SOX9. Cell proliferation ability and cytotoxicity of inhibiting SOX9 were assessed by 3-(4, 5-dimethylthiazolyl-2)-2, 5-diphenyltetrazolium bromide (MTT) and clonogenic assays. The effect of SOX9 knockdown on chordoma cell motility was evaluated by a wound healing assay and a transwell invasion chamber assay. Knockdown of SOX9 induced apoptosis, cell cycle arrest as well as decreased expression of cancer stem cell markers were determined by Western blot and flow cytometric assays. The effect of the combination of SOX9 siRNA and the chemotherapeutic drug doxorubicin/cisplatin on chordoma cells was assessed by a MTT assay.

Results—Tissue microarray (TMA) and IHC analysis showed that SOX9 is broadly expressed in chordomas and that higher expression levels of SOX9 correlated with a poor prognosis. RNA interference (RNAi)-mediated knockdown of SOX9 inhibited chordoma cell growth, decreased cell motility, and induced apoptosis as well as cell cycle arrest. Moreover, the combination of SOX9 inhibition and chemotherapeutic drugs had an enhanced anti-cancer effect on chordoma cells.

Conclusions—Our results demonstrate that SOX9 plays a crucial role in chordoma. Targeting SOX9 provides a new rationale for treatment of chordoma.

Keywords

SOX9; Chordoma; Proliferation; Motility; Apoptosis; Cell cycle

Corresponding author: Zhenfeng Duan, Sarcoma Biology Laboratory, Department of Orthopaedic Surgery, Massachusetts General Hospital and Harvard Medical School, 55 Fruit Street, Jackson 1115, Boston, Massachusetts 02114. Tel: 617-724-3144; Fax: 617-726-3883; zduan@mgh.harvard.edu.

Introduction

Chordomas are rare malignant tumors of the axial skeleton that arise from transformed remnants of notochord (1, 2). The incidence of intra- and extra- cranial chordoma is 0.84 per million population, and chordoma is responsible for approximately 1–4% of all bone tumors (3–5). This disease is most prevalent in the 50 to 60 year age group, and its predilection sites include the skull base (32%), sacrum (29.2%), and mobile spine (32.8%) (4). Surgical resection remains the primary standard of treatment for chordoma patients, which is sometimes combined with radiation therapy. Chordomas are characteristically largely unresponsive to conventional cytotoxic chemotherapy drugs. Currently, there are no specific drugs for chordomas approved by the Food and Drug Administration (FDA) (6). Prognosis and quality of life have remained poor due to limited treatment options. The median survival is 6.29 years, and the overall 5-, 10- and 20 year relative survival rates are 67.6%, 39.9% and 13.1%, respectively (4). There is an urgent need to identify novel therapeutic strategies that can enhance patient outcomes.

SOX9—a high mobility group box (HMG-box) transcription factor—belongs to the SOX family, which includes 20 genes that are classified into nine subgroups according to homology within the HMG domain as well as other structural characteristics and functions (7). The SOX families are involved in embryonic development, sex determination, human genetic syndromes and malignancies (8). SOX9 plays critical roles in embryogenesis, male sexual development, organ development, chondrocyte differentiation, and stem cell properties (9–12). Aberrant constitutive activation of some signaling resulting in the overexpression of SOX9 has been found in many types of solid tumors and the following pathways: the Wnt/ β -catenin pathway increased SOX9 expression in colon, prostate, breast cancer (13–15); the sonic hedgehog (Shh) signaling-Gli2 pathway caused over-activation of SOX9 in skin basal cell carcinoma (16); Notch1 signaling upregulated SOX9 in lung and esophageal adenocarcinoma (17, 18); epidermal growth factor receptor (EGFR) - extracellular signal–regulated kinases 1/2 (ERK1/2) signaling pathway elevated SOX9 expression in urothelial cancer (19); and the NF- κ B signaling pathway positively regulated SOX9 in pancreatic cancer (20). Yet to be discovered are the roles of SOX9 in chordoma as well as the efficacy of targeting SOX9 signaling for treatment. Therefore, we examined the expression of SOX9 in chordoma patient tissues. We also evaluated the function of SOX9 in the proliferation and motility of chordoma cells. In addition, we assessed a potential mechanism for targeting SOX9 inhibition of cell proliferation.

Materials and methods

Human chordoma tumor tissues

Fifty of the chordoma tissue samples (Tissue 1–Tissue 50) were obtained from the Massachusetts General Hospital Sarcoma Tissue Bank and were used in accordance with the policies of the institutional review board of the hospital (IRB protocol # 2007P-002464) and in accordance with common rules by the U.S. Department of Health and Human Services. Written informed consent was obtained from all patients whose specimens and clinical information were used for this research study. All tissue diagnoses were confirmed

histologically. The data collected per patient includes: age, gender, metastasis, recurrence, tumor location(s), months of follow-up, and disease status (Supplementary Table 1).

Chordoma tissue microarray (TMA) and immunohistochemistry (IHC)

Pathologically confirmed chordoma tissues were obtained from patients who had undergone surgical resection in Massachusetts General Hospital, and were conducted according to the policies of the institutional review board of the hospital (IRB protocol # 2007P-002464). A retrospective study that included 50 samples from 50 chordoma patients was identified for the tissue TMA immunohistochemical staining. The expression level of SOX9 was determined based on the Immunohistochemistry Protocol (Paraffin) from Cell Signaling Technology (Danvers, MA). Briefly, each paraffin embedded slide was baked at 60°C for 1 hour. Each section was washed three times in xylene for 5 minutes, and then transferred through graded ethanol (100% and 95%) twice for 10 minutes. Following the process of antigen retrieval, endogenous peroxidase activity was quenched by incubation in 3% hydrogen peroxide. After protein blocking with normal goat serum for 1 hour at room temperature, the SOX9 primary antibody (Sox-9 (H-90): sc-20095, Santa Cruz Biotechnology, 1:50 dilution) was applied at 4°C overnight in a humidified chamber. The bound antibody on the array was detected by using SignalStain®Boost Detection Reagent and SignalStain® DAB (Cell Signaling Technology). Prior to imaging, the section was counterstained with hematoxylin QS (Vector Laboratories) and mounted with VectaMount AQ (Vector Laboratories) coverslip for long-term preservation.

The degree of immunostaining on the tissue array was viewed and scored separately by two independent investigators who had no knowledge of the sample's histopathological features or patient medical history. A joint review of the slides followed by discussion among two investigators was done to reach a consensus that resolved any differences in the scores. The immunostaining intensity pattern of SOX9 was assessed on a semi-quantitative scale defined as follows: a score of 1 indicates 0–25% positive nuclear stained cells; a score of 2 indicates 26–50% positive cells; a score of 3 indicates 51–75% positive cells; a score of 4 indicates 76–100% positive cells (21). Chordoma patients were then subdivided into three SOX9 expression groups: low expression group (SOX9 staining score 1–2: nuclear positive staining 0–50%), moderate expression group (SOX9 staining score 3, nuclear positive staining 51–75%), high expression group (SOX9 staining score 4, nuclear positive staining 76–100%). Light microscopic images were documented using a Nikon Eclipse Ti-U fluorescence microscope (Nikon, New York, NY) with an attached SPOT RT digital camera (Diagnostic Instruments).

Cell lines and cell culture

The human chordoma cell line U-CH1 was established and kindly provided by Dr. Silke Brüderlein (University Hospitals of Ulm, Germany) (22). CH22, another human chordoma cell line, was established in our laboratory as previously reported (23). All cell lines used in this study have been tested and shown to be free of mycoplasma and bacterial. All cell lines were short tandem repeat authenticated within 6 months of use. Both chordoma cell lines were maintained at low passage numbers and cultured in DMEM medium (Life Technologies, Grand Island, NY) supplemented with 10% fetal bovine serum (FBS) (Sigma-

Aldrich, St. Louis, MO), penicillin (100 mg/ml), and streptomycin (100 mg/ml; Invitrogen, Grand Island, NY). All cells were maintained in a humidified incubator containing 5% CO₂ and 95% air atmosphere at 37°C.

Knockdown of SOX9 by RNA interference

SOX9 knockdown in human chordoma cells was performed by siRNA transfection. The human non-specific siRNA oligonucleotides (MISSION[®] siRNA Universal Negative Control, SIC001, Sigma-Aldrich, St. Louis, MO) were used as negative controls. 2×10⁵ chordoma cells per well were seeded in 12-well plates with complete growth medium without antibiotics. Various concentrations (0, 20, 40, and 60 nM) of synthetic human SOX9 siRNA (SASI_Hs01_00240733, the target sequence for human SOX9 siRNA: CGTGTGATCAGTGTGCTAA, coding regions sense 5' - CGUGUGAUCAGUGUGCUAAdTdT-3', antisense 5' - UUAGCACACUGAUCACACGdTdT-3', Sigma-Aldrich, St. Louis, MO) or non-specific siRNA (40nM) were transfected into cells using Lipofectamine RNAiMax Reagent (Invitrogen, CA) according to the manufacturer's instructions.

Cell proliferation assay and clonogenic assay

Cells were exposed to various concentrations of SOX9 siRNA or vehicle control for respective time points as indicated. Cell proliferation ability and cytotoxicity of inhibiting SOX9 were assessed by MTT assays. In brief, chordoma cells were seeded at 3×10³ cells per well into 96-well plates with complete growth medium without antibiotics in duplicate, and treatment with human non-specific siRNA and synthetic human SOX9 siRNA at concentrations ranging from 10 to 80 nM for five days or SOX9 siRNA 20 nM for 1, 2, 3, 4, or 5 days, respectively. Subsequently, 20 µl MTT (Sigma-Aldrich, St. Louis, MO) was added to each well and then incubated for 4 hours at 37°C and 5% CO₂ humidified atmosphere. Then, the MTT formazan product was dissolved with acid isopropanol. The absorbance was assessed on a SpectraMax Microplate[®] Spectrophotometer (Molecular Devices LLC, Sunnyvale, CA) at 490 nm. The MTT assays were performed in triplicate as mentioned above. For clonogenic assays, U-CH1 and CH22 cells were plated at 2×10² cells per well into 6-well plates after transfection with SOX9 siRNA/non-specific siRNA for 48 hours. Cultured with complete growth medium without antibiotics at 37°C for 1–2 weeks, then methanol fixed and Giemsa stained (GS, Sigma-Aldrich, St. Louis, MO), which was followed by colony counting. The clonogenic assay was conducted in duplicate.

Wound healing assay and cell invasion assay

Cell migration activity was evaluated by a wound healing assay. In brief, 2×10⁵ cells were seeded onto 12-well plates and treated with different concentrations of SOX9 siRNA or non-specific siRNA. After the cells reached 100% confluence, they were wounded by scraping three parallel lines with a 200 µl tip, and then washed three times in serum-free medium and incubated in regular medium. Wounds were observed at 0, 8, 24, and 48 hours, respectively. Three images were taken per well at each time point using a Nikon microscope (10× objective) to monitor the cell repair process, and the distance between the two edges of the scratch (wound width) was measured at three random sites in each image. The cell migration distance was calculated by subtracting the wound width at each time point from the wound

width at the 0 hour time point. The wound healing assay was conducted in triplicate. Transwell invasion chamber assay provided an *in vitro* system to study cell invasion activity with a BD BioCoat™ Matrigel™ Invasion Chamber (Becton-Dickinson, MA). In brief, cell suspensions were prepared containing 5×10^4 cells per well in the upper chambers of 24 well invasion chambers with serum-free medium, while the bottom chambers were filled with 750 μ l of medium with 10% FBS without antibiotics. After a 48 hours treatment with SOX9 siRNA or non-specific siRNA, the non-invading cells were carefully scrubbed from the upper surface of the membrane with a cotton swab. Cells were fixed using 100% methanol, stained in hematoxylin for 15 minutes, and rinsed twice in distilled water. The numbers of invading cells were counted in three images per membrane under a microscope using a 20 \times objective. The transwell invasion chamber assay was performed in duplicate.

Protein preparing and Western blotting

Protein lysates of the cells were extracted with 1 \times RIPA lysis buffer (Upstate Biotechnology, Charlottesville, VA) supplemented with complete protease inhibitor cocktail tablets (Roche Applied Science, IN, USA) after incubation with SOX9 siRNA/non-specific siRNA for 48 hours. Western blotting was performed as follows: denatured proteins were run on NuPAGE® 4–12% Bis-Tris Gel (Life Technologies), and then transferred to a nitrocellulose membrane (Bio-Rad). Membranes were blocked in 5% nonfat milk for 1 hour, and incubated with specific primary antibody (Sox-9 (H-90): sc-20095, Santa Cruz Biotechnology, 1:1000 dilution) or mouse monoclonal antibody to human β -actin (Sigma-Aldrich, St. Louis, MO, USA) at 4°C overnight. Following primary antibody incubation, membranes were washed with PBST (1 \times), and goat anti-rabbit IRDye® 800CW or goat anti-mouse IRDye® 680LT secondary antibody (1:20000 dilution) (926-32211 and 926-68020, Li-COR Biosciences, NE, USA) were added, respectively. Bands were detected using Odyssey for Infrared Fluorescent Western Blots from Li-COR Bioscience (Lincoln, NE, USA). Quantification analysis of Western blot bands was performed with ImageJ software (National Institutes of Health, USA). All primary antibodies used in this study are described in Supplementary Table 3. The Western blot assay was conducted in duplicate.

Immunofluorescence

Expressions of SOX9 and p21 protein were also evaluated by immunofluorescence. In brief, cells were transfected with SOX9 siRNA/non-specific siRNA for 48 hours. Then the cells were incubated in 4% paraformaldehyde, fixed in ice-cold methanol, blocked with 1% bovine serum albumin (BSA), and were bound to SOX9 (1:50), p21 (1:50) and actin (1:400) antibodies at 4°C overnight. Then, the cells were incubated with anti-rabbit IgG (1:1,000), anti-mouse IgG (1:1,000) and Hoechst 33342 (Life Technologies Corp., NY).

Analysis of cells by flow cytometry assays

Cells were exposed to SOX9 siRNA/non-specific siRNA for 48 hours and harvested per manufacturer protocols. For apoptosis, cells were washed twice with cold PBS and then resuspended in 1 \times Binding Buffer (BD Biosciences, San Diego, CA) at a concentration of 1×10^6 cells/ml. 100 μ l of the solution (1×10^5 cells) was transferred to a 5 ml culture tube, and 5 μ l of FITC Annexin V (BD Biosciences) was added. Then, 10 μ l of propidium iodide (PI) (BD Biosciences) was added, the cells were vortexed and subsequently incubated for 15

min at room temperature (25 °C) in the dark. 400 µl of 1× Binding Buffer was added to each tube, and the cells were analyzed by flow cytometry (BD FACSCalibur, BD Biosciences). For cell cycle analysis, the collected cells were fixed in 70% ethanol for 24 hours, washed with PBS, and stained with 20 µg/ml PI in the presence of 1µg/ml RNase (type IIA, Sigma-Aldrich, St. Louis, MO) in PBS. After 15 minutes of incubation, cells were collected on an LSR II cytometer using the 488-nm excitation line running DIVA acquisition software (BD, Franklin Lakes, NJ). Before analysis, instrument linearity was checked with PI-labeled chicken erythrocyte nuclei and BD DNA QC particles. Doublets were excluded with PI area versus width analysis. Cell cycle analysis was performed on list-mode data files with FlowJo cell cycle analysis software (Tree Star, Inc., Ashland, OR). The flow cytometry assays mentioned above were performed in duplicate or triplicate.

Inhibition of SOX9 in combination with chemotherapy in chordoma cell lines

The effect of the combination of SOX9 siRNA and the chemotherapeutic drug doxorubicin/cisplatin on chordoma cells was assessed by a MTT assay. The cells were seeded into 96-well plates at a density of 3×10^3 cells per well and incubated with a series of concentrations of doxorubicin/cisplatin (supplied by the pharmacy at the Massachusetts General Hospital) and 10nM SOX9 siRNA for five days. After five days of co-incubation, cell proliferation was determined by the MTT assay as previously described. The MTT assay was conducted in triplicate.

Statistical analysis

The data was analyzed using Prism 6.0 software (Graph Pad Software Inc., San Diego, CA), and expressed as mean \pm SD. Statistical significance was assessed using independent two-tailed Student t-tests for independent data. One-way ANOVA tests were performed for multiple comparisons. Associations between results of IHC and clinicopathological factors were assessed by the Chi-square test. Survival analysis was performed using Kaplan-Meier survival curves with a Log-rank test for significance. Differences of $P < 0.05$ were considered significant for all statistical tests.

Results

SOX9 is expressed in human chordoma tissues and associated with poor prognosis

In this study, fifty patients with pathological diagnosis of chordoma were identified (Supplementary Table 1). The summary of the clinicopathological characteristics of chordoma patients is shown in Supplementary Table 2. We examined the expression of SOX9 in these chordoma tissues. Of the 50 patients with chordoma, forty-nine (98%) patients were classified with a SOX9 positive stain while only one patient (2%) had a SOX9 negative stain. The results demonstrated that the SOX9 protein was broadly expressed in patients with chordoma (Fig. 1A). However, there was no significant difference in SOX9 expression despite differences in age, gender, and tumor location, origin, and margin of resection (Supplementary Table 2). In addition, the results also showed that the SOX9 protein was predominantly localized in the nucleus of chordoma cells (Fig. 1A).

To explore the relationship between SOX9 expression and clinical prognosis, we evaluated SOX9 staining in chordoma patient specimens. With respect to clinical characteristics, recurrence is a major concern in chordoma patient management and is associated with poor survival and quality of life and marked morbidity. Moreover, the disease-free survival is an important approach to measure how well a new treatment works in a clinical trial. Therefore, we assessed disease-free survival times between the two staining groups: low (SOX9 staining scores 1–2, n = 24) and high (SOX9 staining score 4, n = 10) expression of SOX9. The median disease-free survival times of the two groups were 154 and 56.5 months, respectively. Kaplan-Meier survival analysis showed that the prognosis for patients with low expression of SOX9 was significantly better than the high expression of SOX9 chordoma patients ($P = 0.0032$) (Fig. 1B). Also, overall survival for chordoma patients with high SOX9 staining was significantly worse than those with low SOX9 staining ($P = 0.0068$) (Fig. 1C). The relatively small number of events precluded disease free and overall survival analysis using three staining groups. Also on Cox Proportional Hazards regression analysis, SOX9 expression in chordoma was a significant risk factor of overall survival (hazard ratio (HR), 0.34; 95% confidence interval (CI), 0.06–0.59; $P=0.0068$), as well as disease-free survival (HR, 0.31; 95% CI, 0.05–0.51; $P=0.0032$) between low and high expression of SOX9 groups.

SOX9 is crucial for chordoma cell growth and survival

To characterize the functional role of SOX9 in chordoma, we investigated the effect of SOX9 knockdown on chordoma cell growth *in vitro* by RNAi. As compared with other types of human cancer cells, chordoma cells usually exhibit specific morphological characteristic of round nucleus with clear vacuolated cytoplasm (also named as physaliphorous cells, Fig. 2A). After incubation with SOX9 siRNA or non-specific siRNA for five days, the inhibition of cell viability effects were observed in both U-CH1 and CH22 cell lines (Fig. 2B). The MTT assay also showed that knockdown of SOX9 significantly reduced chordoma cell viability and proliferation in both cell lines in a dose-dependent manner (Fig. 2C).

To further evaluate the time-specific effect of SOX9 knockdown on chordoma cells, we then treated both chordoma cell lines with 20 nM SOX9 siRNA or non-specific siRNA for 24, 48, 72, 96, and 120 hours, respectively. The MTT assay revealed that both U-CH1 and CH22 chordoma cell lines showed striking growth hampered at 48 hours after transfection with SOX9 siRNA (Fig. 2D). In contrast, control and non-specific siRNA transfected cells showed no effects on growth during the observation period (Fig. 2D).

To demonstrate the specificity of the inhibitory impact of SOX9 knockdown on survival and proliferation capacity of chordoma cells, we next analyzed the ability of cells to form colonies after transfection SOX9 siRNA. As shown in Figure 2E and Figure 2F, the colonies were significantly reduced in both SOX9 siRNA treated cell lines.

Downregulated expression of SOX9 was also confirmed by Western blot and immunofluorescence assays in both U-CH1 (Fig. 3A, Fig. 3C) and CH22 (Fig. 3B, Fig. 3D), respectively. The level of SOX9 expression suppressed by SOX9 targeted siRNA showed in a dose-dependent manner, as determined by densitometry quantification of Western blots (top panels of Fig. 3A and Fig. 3B). Brachyury, a specific biomarker for chordomas, was

consistently identified in both cell lines and showed no alteration (second panels of Fig. 3A and Fig. 3B) after SOX9 knock down (24). These results indicate that SOX9 is a vital regulator of cell growth and viability in chordomas.

Inhibition of SOX9 suppresses chordoma cell motility

Chordoma is aggressively invasive hence we examined the influence of SOX9 inhibition on chordoma cell migration and invasion since cell motility plays a fundamental role in tumor invasion and metastasis (25). We observed a significant attenuation of migratory potential in both U-CH1 and CH22 cell lines compared with control or non-specific siRNA groups, especially at higher concentrations of SOX9 siRNA treated groups (Fig. 4A and 4B). Wounds almost fully recovered after the 48-hour migration period experienced by cells in the blank control and non-specific siRNA treated groups. In parallel, the invasive ability of both cell lines was markedly reduced after treatment with SOX9 siRNA, which was assessed in transwell invasion chamber assays (Fig. 4C and 4D). Considered together, the data confirms that the inhibition of SOX9 results in impaired ability of chordoma cell motility.

SOX9 inhibition induces apoptosis and cycle arrest in chordoma cells

To explore the possible causes of the observed inhibitory effect on chordoma cell growth and motility induced by SOX9 inhibition, we examined apoptosis associated proteins in SOX9 siRNA treated chordoma cells. As shown in Figure 5A, downregulation of anti-apoptotic proteins (Bcl-xL and survivin) were observed at SOX9 siRNA treated cells compared with controls or non-specific siRNA treatments. As also depicted in Figure 5A, concentration levels of the following proteins also decreased: cell cycle-related proteins [cyclin D1 and phosphorylated retinoblastoma protein (pRb)]; protein response to DNA damage [Checkpoint kinase 1 (Chk1)]; proteins involved in cell migration [Slug and matrix metalloproteinase 9 (MMP-9)]; and cancer stem cell markers (Nanog and c-Myc). Notably, a potent cyclin-dependent kinase (CDK) inhibitor, p21, had higher concentrations in both cell lines treated with SOX9 siRNA than the controls or non-specific siRNA treatment groups (Fig. 5A and 5B). Upregulation of p21 was further confirmed by an immunofluorescence assay (Fig. 5C and 5D).

To validate Western blot results and further explore the potential mechanism underlying inhibiting effects on the growth of chordoma cells, we also performed flow cytometric assays. Both chordoma cell lines showed markedly increased rates of apoptosis in a dose-dependent fashion compared with the controls (Fig. 6A and 6B). To determine the specific impact of SOX9 inhibition on the cell cycle of tumor cells, we further assessed cell cycle phase distributions in both chordoma cell lines. As depicted in Figures 6C and 6D, following treatment with SOX9 siRNA, the number of cells in G1 phase significantly increased, whereas a decrease of the number of cells in S phase occurred in both U-CH1 and CH22 cell lines in comparison with control cells. This data suggests that there is diminished chordoma cell growth as a result of the inhibition of SOX9 induced apoptosis and G1-phase cell cycle arrest.

SOX9 inhibition combined with chemotherapy

To investigate how the growth of chordoma cells is effected by the combination of SOX9 inhibition and the conventional chemotherapy agent doxorubicin/cisplatin, both U-CH1 and CH22 cell lines were co-treated with increasing doses of doxorubicin/cisplatin and SOX9 siRNA 10 nM for five days. As measured by MTT analysis, both chordoma cell lines showed only a possible modest increase in anti-cancer effects due to the combination of doxorubicin or cisplatin with SOX9 siRNA (Supplementary Fig. S1A and S1B).

Discussion

This is the first study that reveals the crucial role of SOX9 in chordoma. Expression of SOX9 protein was observed in the majority of chordomas. High expression of SOX9 is correlated with a worse prognosis for patients with chordomas. Lower expression of the SOX9 protein group has a better prognosis in terms of overall survival and disease-free survival. As described in previous reports, our findings confirmed that the overexpression of SOX9 in certain cancers is associated with poor prognosis (12, 17, 26–28). The functional roles of SOX9 were evaluated *in vitro*, and the results showed that the knockdown of SOX9 abolished proliferation in chordoma cells, suppressed cell motility, induced apoptosis and cell cycle arrest. Chemotherapy drug sensitivity was only modestly enhanced, perhaps not surprisingly given the almost total lack of chemotherapy effect in chordoma. These results suggest that SOX9 could play a critical role in maintaining chordoma cell growth and proliferation.

SOX9 and brachyury both belong to a subset of mesodermal genes and play a critical role in the embryonic, axial skeleton and notochord development. Both SOX9 and brachyury are expressed in the notochord, but the functional role of SOX9 in maintaining the notochord is not directly regulated by brachyury (29–31). SOX9 expression cannot be referenced during a diagnosis to distinguish between a chordoma and a chondrosarcoma since it is overexpressed in both. Brachyury has been identified as a definitive diagnostic biomarker of chordoma, which is only expressed in chordomas and not detected in any other sarcoma (24, 32). We demonstrated that the knockdown of SOX9 expression had no effect on the expression level of brachyury in chordoma cells, indicating that SOX9 may not act upstream of brachyury, which coincides with previous reports (30).

Considering the analysis of flow cytometric data alongside the decreased expression levels of anti-apoptotic proteins—including survivin and Bcl-xL, the knockdown of SOX9 reveals its involvement in apoptosis signaling. Survivin belongs to the inhibitor of apoptosis (IAP) gene family and has an anti-apoptotic effect when it directly binds to caspase-3, a critical effector of apoptosis, which inhibits caspase-3 activation (33). It is important to note that survivin is also expressed in chordoma patient specimens and that the inhibition of survivin prevented chordoma cell growth (34). Moreover, the knockdown of survivin by RNAi reduced the clonogenic survival of human sarcoma cells (35). Bcl-xL is a member of the Bcl-2 family of proteins—another well-established key regulator of the apoptosis gene family. Bcl-xL induces a cell survival function in response to apoptotic stimuli through the mechanism of decreased mitochondrial permeability and the inhibition of mitochondrial cytochrome c release, which subsequently activates caspase and Poly(ADP-ribose)

polymerase (PARP) cleavage in the apoptosis pathway (36). p21, a potent CDK inhibitor, leads to cell cycle arrest at specific stages. Depending on the cellular context and circumstances, particularly in the intracellular localization, p21 functions as a tumor suppressor or as an oncogene (37, 38). According to the results of Western blot and immunofluorescence assays, we discovered that SOX9 inhibition results in increased p21 expression levels and also nuclear accumulation in both chordoma cell lines. These findings were consistent with a previous report describing that the knockdown of SOX9 leads to an upregulation of p21 in lung adenocarcinoma (39). Subsequently, cell cycle arrest was facilitated by an upregulation of the p21 blockade cyclin/CDKs complexes working as CDK inhibitors in addition to a decrease of the pRb transcription factor (Supplementary Fig. S2). SOX9 inhibition in chordoma cells also caused a reduction in the expression levels of cyclin D1—another vital protein for the G1/S cell cycle transition. The overexpression of cyclin D1 gives it a well-documented reputation as an oncogene heavily involved in the progression of various cancer types as well as a link to poor prognosis (40). Rb is a tumor suppressor protein and dysregulation of Rb leads to oncogenic phenotypes in several major cancers (41). Rb becomes inactive and allows cell cycle progression from the G1 phase to the S phase upon phosphorylation by CDKs. Consequently, pRb promotes cell cycle progression. Knockdown of SOX9 also resulted in decreased pRb in both chordoma cell lines. Indeed, previous studies found that abnormalities of cyclin D1 and pRb were both implicated in tumorigenic features of chordoma (42). Taken together, our study demonstrated that the inhibition of SOX9 induces apoptosis and cell cycle arrest in chordoma cells.

Radiation and chemotherapy resistance are in great part due to tumor cells that have the ability to tolerate DNA damage responses. We found that Chk1 was downregulated in both chordoma cell lines, which is vital to the DNA damage response and the proper functioning of the cell cycle checkpoints (43). Given that Chk1 inhibition enhances cancers sensitive to radiation and chemotherapy, our findings suggest that targeting SOX9 may enable a desired response to chemotherapy or alleviate heavy radiation required for the treatment of chordoma patients (43, 44).

Slug—a member of the Snail family of C2H2-type zinc finger transcription factors—is characterized by its role in the epithelial-mesenchymal transition (EMT), which has phenotypic crossover with tumor cells, including: invasion, migration, metastasis, and therapy resistance. Overexpression of Slug has been reported in lung cancer, aggressive chordomas, and promotion of tumor cell invasion (45, 46). MMP-9 also plays a central role in cancer invasion and metastasis progression by extracellular matrix remodeling and angiogenesis (47). Targeting MMP-9 decreased the capacity of malignant meningioma cell growth, invasion and angiogenesis (48). More specifically, a recent study found that MMP-9 is ubiquitously expressed in primary and recurrent chordoma specimens (49). In line with these findings, we observed that chordoma cell motility decreased with the knockdown of SOX9 in addition to the downregulation of Slug and MMP-9.

There is strong evidence that SOX9 is a vital factor contributing to the malignant properties of cancer stem cells (12, 20, 28, 50). More importantly, chordoma cells have been coupled with cancer stem-like cells due to their similarities in the following characteristics: chemotherapy resistance, tendency for recurrence, and metastasis (51). We observed SOX9

knockdown resulted in reduced expression of cancer stem cell markers Nanog and c-Myc. More interestingly, p21 could inhibit c-Myc induced features of EMT in human breast cancer cells (52). Further research unraveling the SOX9-mediated mechanisms underlying the cancer stem-like cell properties in chordoma may lead to advances in treating this rare disease (51).

Finally, we found that the inhibition of SOX9 with siRNA enhanced the cytotoxic effect of doxorubicin/cisplatin in chordoma cells, which is consistent with a previous report that the knockdown of SOX9 sensitized ovarian cancer cells to paclitaxel and cisplatin (53). This data suggests that a combination therapy of SOX9 inhibition and chemotherapy drugs could be considered for clinical trials as a potent treatment for chordoma patients.

No data from clinical trials regarding the inhibition of SOX9 in human chordoma patients is available. However, given the important role of SOX9 in different cancers including chordomas, further refinements to and knowledge of its signaling pathways will lead to novel cancer therapy approaches.

In conclusion, our study reveals that SOX9 is broadly expressed in chordomas. High expression of SOX9 is associated with poor outcomes, which may serve as a prognostic and predictive biomarker in chordoma patients. Inhibition of SOX9 results in significantly decreased cell growth and motility in chordoma. This effect was enhanced when combined with chemotherapeutic drugs. Our observations are a novel insight into the role of SOX9 in chordoma and provide a new rationale for targeting SOX9 in the treatment of chordoma. Further studies of the molecular mechanisms of SOX9 in chordoma and *in vivo* investigation should be explored.

Supplementary Material

Refer to Web version on PubMed Central for supplementary material.

Acknowledgments

Financial support for authors: This project was partially supported by grants from the Stephan L. Harris Fund, and the Gattegno and Wechsler funds. Support was also provided by the Chordoma Foundation. Dr. Duan is supported, in part, through a grant from the Sarcoma Foundation of America (SFA), a grant from the National Cancer Institute (NCI)/National Institutes of Health (NIH), UO1, CA151452-01, a pilot grant from Sarcoma SPORE/NIH, and a grant from an Academic Enrichment Fund of MGH Orthopedic Surgery.

Abbreviations

SOX9	sex-determining region Y (SRY)-box 9
RNAi	RNA interference
MTT	3-(4, 5-dimethylthiazolyl-2)-2, 5-diphenyltetrazolium bromide
HMG-box	high mobility group box
Shh	sonic hedgehog
EGFR	epidermal growth factor receptor

ERK1/2	extracellular signal-regulated kinases 1/2
TMA	tissue microarray
IHC	immunohistochemistry
FBS	fetal bovine serum
BSA	bovine serum albumin
PI	propidium iodide
HR	hazard ratio
CI	confidence interval
pRb	phosphorylated retinoblastoma protein
Chk1	checkpoint kinase 1
MMP-9	matrix metalloproteinase 9
CDK	cyclin-dependent kinase
IAP	inhibitor of apoptosis
PARP	Poly(ADP-ribose) polymerase
EMT	epithelial-mesenchymal transition

References

1. Yamaguchi T, Yamato M, Saotome K. First histologically confirmed case of a classic chordoma arising in a precursor benign notochordal lesion: differential diagnosis of benign and malignant notochordal lesions. *Skeletal radiology*. 2002; 31:413–8. [PubMed: 12107574]
2. Deshpande V, Nielsen GP, Rosenthal DI, Rosenberg AE. Intraosseous benign notochord cell tumors (BNCT): further evidence supporting a relationship to chordoma. *The American journal of surgical pathology*. 2007; 31:1573–7. [PubMed: 17895760]
3. Smoll NR, Gautschi OP, Radovanovic I, Schaller K, Weber DC. Incidence and relative survival of chordomas. *Cancer*. 2013; 119:2029–37. [PubMed: 23504991]
4. McMaster ML, Goldstein AM, Bromley CM, Ishibe N, Parry DM. Chordoma: incidence and survival patterns in the United States, 1973–1995. *Cancer Causes & Control*. 2001; 12:1–11. [PubMed: 11227920]
5. Fletcher CD, Unni KK, Mertens F. *Pathology and genetics of tumours of soft tissue and bone*: Iarc. 2002
6. Walcott BP, Nahed BV, Mohyeldin A, Coumans J-V, Kahle KT, Ferreira MJ. Chordoma: current concepts, management, and future directions. *The lancet oncology*. 2012; 13:e69–e76. [PubMed: 22300861]
7. Bowles J, Schepers G, Koopman P. Phylogeny of the SOX family of developmental transcription factors based on sequence and structural indicators. *Developmental biology*. 2000; 227:239–55. [PubMed: 11071752]
8. Castillo SD, Sanchez-Cespedes M. The SOX family of genes in cancer development: biological relevance and opportunities for therapy. *Expert opinion on therapeutic targets*. 2012; 16:903–19. [PubMed: 22834733]

9. Wagner T, Wirth J, Meyer J, Zabel B, Held M, Zimmer J, et al. Autosomal sex reversal and campomelic dysplasia are caused by mutations in and around the SRY-related gene SOX9. *Cell*. 1994; 79:1111–20. [PubMed: 8001137]
10. Akiyama H, Chaboissier M-C, Martin JF, Schedl A, de Crombrugge B. The transcription factor Sox9 has essential roles in successive steps of the chondrocyte differentiation pathway and is required for expression of Sox5 and Sox6. *Genes & development*. 2002; 16:2813–28. [PubMed: 12414734]
11. Bell DM, Leung K, Wheatley SC, Ng LJ, Zhou S, Ling KW, et al. SOX9 directly regulates the Type 2 collagen gene. *Nat Genet*. 1997; 16:174–8. [PubMed: 9171829]
12. Guo W, Keckesova Z, Donaher JL, Shibue T, Tischler V, Reinhardt F, et al. Slug and Sox9 cooperatively determine the mammary stem cell state. *Cell*. 2012; 148:1015–28. [PubMed: 22385965]
13. Blache P, Van de Wetering M, Duluc I, Domon C, Berta P, Freund J-N, et al. SOX9 is an intestine crypt transcription factor, is regulated by the Wnt pathway, and represses the CDX2 and MUC2 genes. *J Cell Biol*. 2004; 166:37–47. [PubMed: 15240568]
14. Wang H, McKnight NC, Zhang T, Lu ML, Balk SP, Yuan X. SOX9 is expressed in normal prostate basal cells and regulates androgen receptor expression in prostate cancer cells. *Cancer research*. 2007; 67:528–36. [PubMed: 17234760]
15. Wang H, He L, Ma F, Regan MM, Balk SP, Richardson AL, et al. SOX9 regulates low density lipoprotein receptor-related protein 6 (LRP6) and T-cell factor 4 (TCF4) expression and Wnt/ β -catenin activation in breast cancer. *Journal of Biological Chemistry*. 2013; 288:6478–87. [PubMed: 23306204]
16. Vidal VP, Chaboissier M-C, Lützkendorf S, Cotsarelis G, Mill P, Hui C-C, et al. Sox9 is essential for outer root sheath differentiation and the formation of the hair stem cell compartment. *Current Biology*. 2005; 15:1340–51. [PubMed: 16085486]
17. Capaccione KM, Hong X, Morgan KM, Liu W, Bishop J, Liu L, et al. Sox9 mediates Notch1-induced mesenchymal features in lung adenocarcinoma. *Oncotarget*. 2014; 5:3636–50. [PubMed: 25004243]
18. Song S, Maru DM, Ajani JA, Chan C-H, Honjo S, Lin H-K, et al. Loss of TGF- β adaptor β 2SP activates notch signaling and SOX9 expression in esophageal adenocarcinoma. *Cancer research*. 2013; 73:2159–69. [PubMed: 23536563]
19. Ling S, Chang X, Schultz L, Lee TK, Chaux A, Marchionni L, et al. An EGFR-ERK-SOX9 signaling cascade links urothelial development and regeneration to cancer. *Cancer research*. 2011; 71:3812–21. [PubMed: 21512138]
20. Sun L, Mathews LA, Cabarcas SM, Zhang X, Yang A, Zhang Y, et al. Epigenetic Regulation of SOX9 by the NF- κ B Signaling Pathway in Pancreatic Cancer Stem Cells. *Stem cells*. 2013; 31:1454–66. [PubMed: 23592398]
21. McDonald J, Pilgram T. Nuclear expression of p53, p21 and cyclin D1 is increased in bronchioloalveolar carcinoma. *Histopathology*. 1999; 34:439–46. [PubMed: 10231419]
22. Scheil S, Bruderlein S, Liehr T, Starke H, Herms J, Schulte M, et al. Genome-wide analysis of sixteen chordomas by comparative genomic hybridization and cytogenetics of the first human chordoma cell line, U-CH1. *Genes, Chromosomes and Cancer*. 2001; 32:203–11. [PubMed: 11579460]
23. Liu X, Nielsen GP, Rosenberg AE, Waterman PR, Yang W, Choy E, et al. Establishment and characterization of a novel chordoma cell line: CH22. *Journal of Orthopaedic Research*. 2012; 30:1666–73. [PubMed: 22504929]
24. Vujovic S, Henderson S, Presneau N, Odell E, Jacques T, Tirabosco R, et al. Brachyury, a crucial regulator of notochordal development, is a novel biomarker for chordomas. *The Journal of pathology*. 2006; 209:157–65. [PubMed: 16538613]
25. Friedl P, Wolf K. Tumour-cell invasion and migration: diversity and escape mechanisms. *Nature Reviews Cancer*. 2003; 3:362–74. [PubMed: 12724734]
26. Wang H, Leav I, Ibaragi S, Wegner M, Hu G-f, Lu ML, et al. SOX9 is expressed in human fetal prostate epithelium and enhances prostate cancer invasion. *Cancer research*. 2008; 68:1625–30. [PubMed: 18339840]

27. Lü B, Fang Y, Xu J, Wang L, Xu F, Xu E, et al. Analysis of SOX9 expression in colorectal cancer. *American journal of clinical pathology*. 2008; 130:897–904. [PubMed: 19019766]
28. Leung CO-N, Mak W-N, Kai AK-L, Chan K-S, Lee TK-W, Ng IO-L, et al. Sox9 confers stemness properties in hepatocellular carcinoma through Frizzled-7 mediated Wnt/ β -catenin signaling. *Oncotarget*. 2016; 7:29371. [PubMed: 27105493]
29. Quintana L, Muiños TF, Genové E, Del Mar Olmos M, Borrós S, Semino CE. Early tissue patterning recreated by mouse embryonic fibroblasts in a three-dimensional environment. *Tissue Engineering Part A*. 2008; 15:45–54.
30. Barrionuevo F, Taketo MM, Scherer G, Kispert A. Sox9 is required for notochord maintenance in mice. *Developmental biology*. 2006; 295:128–40. [PubMed: 16678811]
31. Nibu Y, José-Edwards DS, Di Gregorio A. From notochord formation to hereditary chordoma: the many roles of Brachyury. *BioMed research international*. 2013; 2013
32. Oakley GJ, Fuhrer K, Seethala RR. Brachyury, SOX-9, and podoplanin, new markers in the skull base chordoma vs chondrosarcoma differential: a tissue microarray-based comparative analysis. *Modern Pathology*. 2008; 21:1461–9. [PubMed: 18820665]
33. Altieri DC. Validating survivin as a cancer therapeutic target. *Nature Reviews Cancer*. 2003; 3:46–54. [PubMed: 12509766]
34. Froehlich EV, Rinner B, Deutsch AJ, Meditz K, Knausz H, Troppan K, et al. Examination of survivin expression in 50 chordoma specimens—a histological and in vitro study. *Journal of Orthopaedic Research*. 2015; 33:771–8. [PubMed: 25640185]
35. Kappler M, Bache M, Bartel F, Kotsch M, Panian M, Würfl P, et al. Knockdown of survivin expression by small interfering RNA reduces the clonogenic survival of human sarcoma cell lines independently of p53. *Cancer gene therapy*. 2004; 11:186–93. [PubMed: 14739938]
36. Finucane DM, Bossy-Wetzel E, Waterhouse NJ, Cotter TG, Green DR. Bax-induced caspase activation and apoptosis via cytochrome c release from mitochondria is inhibitable by Bcl-xL. *Journal of Biological Chemistry*. 1999; 274:2225–33. [PubMed: 9890985]
37. Abbas T, Dutta A. p21 in cancer: intricate networks and multiple activities. *Nature Reviews Cancer*. 2009; 9:400–14. [PubMed: 19440234]
38. Warfel NA, El-Deiry WS. p21WAF1 and tumorigenesis: 20 years after. *Current opinion in oncology*. 2013; 25:52–8. [PubMed: 23159848]
39. Jiang SS, Fang W-T, Hou Y-H, Huang S-F, Yen BL, Chang J-L, et al. Upregulation of SOX9 in lung adenocarcinoma and its involvement in the regulation of cell growth and tumorigenicity. *Clinical Cancer Research*. 2010; 16:4363–73. [PubMed: 20651055]
40. Musgrove EA, Caldon CE, Barraclough J, Stone A, Sutherland RL. Cyclin D as a therapeutic target in cancer. *Nature Reviews Cancer*. 2011; 11:558–72. [PubMed: 21734724]
41. Giacinti C, Giordano A. RB and cell cycle progression. *Oncogene*. 2006; 25:5220–7. [PubMed: 16936740]
42. Naka T, Boltze C, Kuester D, Schulz TO, Schneider-Stock R, Kellner A, et al. Alterations of G1-S checkpoint in chordoma. *Cancer*. 2005; 104:1255–63. [PubMed: 16078265]
43. Smith J, Mun Tho L, Xu N, Gillespie DA. The ATM-Chk2 and ATR-Chk1 pathways in DNA damage signaling and cancer. *Advances in cancer research*. 2010; 108:73–112. [PubMed: 21034966]
44. Bao S, Wu Q, McLendon RE, Hao Y, Shi Q, Hjelmeland AB, et al. Glioma stem cells promote radioresistance by preferential activation of the DNA damage response. *nature*. 2006; 444:756–60. [PubMed: 17051156]
45. Shih J-Y, Tsai M-F, Chang T-H, Chang Y-L, Yuan A, Yu C-J, et al. Transcription repressor slug promotes carcinoma invasion and predicts outcome of patients with lung adenocarcinoma. *Clinical Cancer Research*. 2005; 11:8070–8. [PubMed: 16299238]
46. Karamchandani J, Wu MY, Das S, Vogel H, Muller P, Cusimano M, et al. Highly proliferative sellar chordoma with unusually rapid recurrence. *Neuropathology*. 2013; 33:424–30. [PubMed: 23082799]
47. Deryugina EI, Quigley JP. Matrix metalloproteinases and tumor metastasis. *Cancer and Metastasis Reviews*. 2006; 25:9–34. [PubMed: 16680569]

48. Tummalapalli P, Spomar D, Gondi CS, Olivero WC, Gujrati M, Dinh DH, et al. RNAi-mediated abrogation of cathepsin B and MMP-9 gene expression in a malignant meningioma cell line leads to decreased tumor growth, invasion and angiogenesis. *International journal of oncology*. 2007; 31:1039–50. [PubMed: 17912429]
49. Froehlich EV, Scheipl S, Lazàry A, Varga PP, Schmid C, Stammberger H, et al. Expression of ezrin, MMP-9, and COX-2 in 50 chordoma specimens: a clinical and immunohistochemical analysis. *Spine*. 2012; 37:E757–E67. [PubMed: 22228328]
50. Luanpitpong S, Li J, Manke A, Brundage K, Ellis E, McLaughlin SL, et al. SLUG is required for SOX9 stabilization and functions to promote cancer stem cells and metastasis in human lung carcinoma. *Oncogene*. 2015
51. Aydemir E, Bayrak OF, Sahin F, Atalay B, Kose GT, Ozen M, et al. Characterization of cancer stem-like cells in chordoma: Laboratory investigation. *Journal of neurosurgery*. 2012; 116:810–20. [PubMed: 22283189]
52. Liu M, Casimiro MC, Wang C, Shirley LA, Jiao X, Katiyar S, et al. p21CIP1 attenuates Ras-and c-Myc-dependent breast tumor epithelial mesenchymal transition and cancer stem cell-like gene expression in vivo. *Proceedings of the National Academy of Sciences*. 2009; 106:19035–9.
53. Raspaglio G, Petrillo M, Martinelli E, Puma DDL, Mariani M, De Donato M, et al. Sox9 and Hif-2 α regulate TUBB3 gene expression and affect ovarian cancer aggressiveness. *Gene*. 2014; 542:173–81. [PubMed: 24661907]

Translational Relevance

Chordoma is a rare cancer that is unresponsive to conventional cytotoxic chemotherapy drugs. Our study reveals a finding not yet discovered previously, which is that the sex-determining region Y (SRY)-box 9 (SOX9) is broadly expressed in 49 (98%) of 50 chordoma tissue samples. High expression of SOX9 is significantly associated with poor disease-free survival and overall survival in chordomas ($P = 0.0032$ and 0.0068 , respectively). Inhibition of SOX9 results in decreased cell growth and motility in chordoma. This effect was enhanced when combined with chemotherapeutic drugs. Furthermore, we demonstrate that RNA interference (RNAi)-mediated knockdown of SOX9 induced apoptosis, cell cycle arrest, and reduced expression of cancer stem cell markers. These findings suggest that SOX9 is a critical component of chordoma cell growth and could be a promising therapeutic target for the treatment of chordomas.

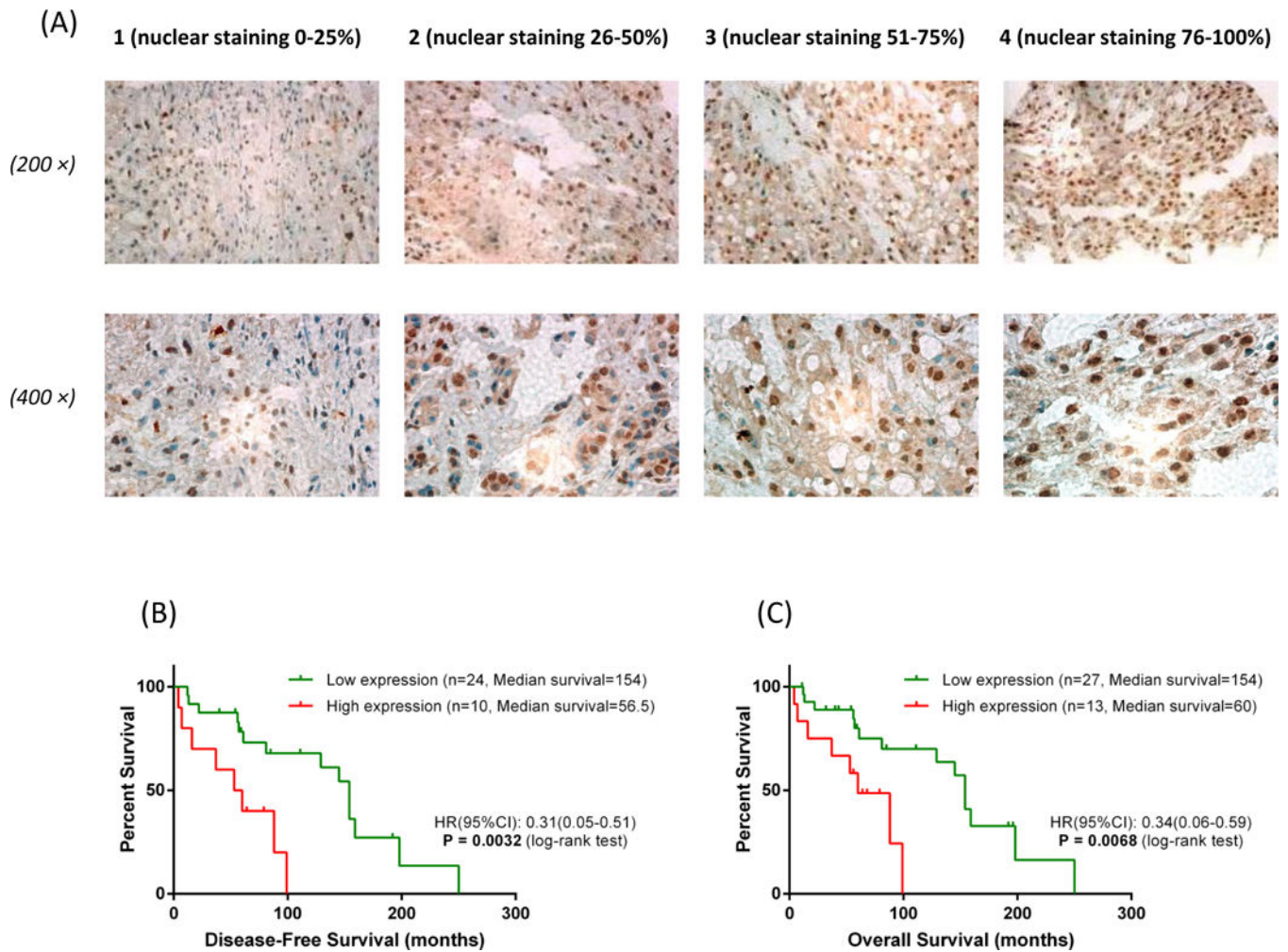


Figure 1.

SOX9 is expressed in chordoma and correlates with poor patient prognosis. (A) Representative images of nuclear staining intensity for SOX9 in human chordoma tumor tissues. Original magnification: 200× and 400×. (B) Correlation between expression of SOX9 (low and high expression) and disease-free survival in chordoma patients by Kaplan-Meier survival curve estimation. (C) Correlation between expression of SOX9 (low and high expression) and overall survival in chordoma patients by Kaplan-Meier survival curve estimation.

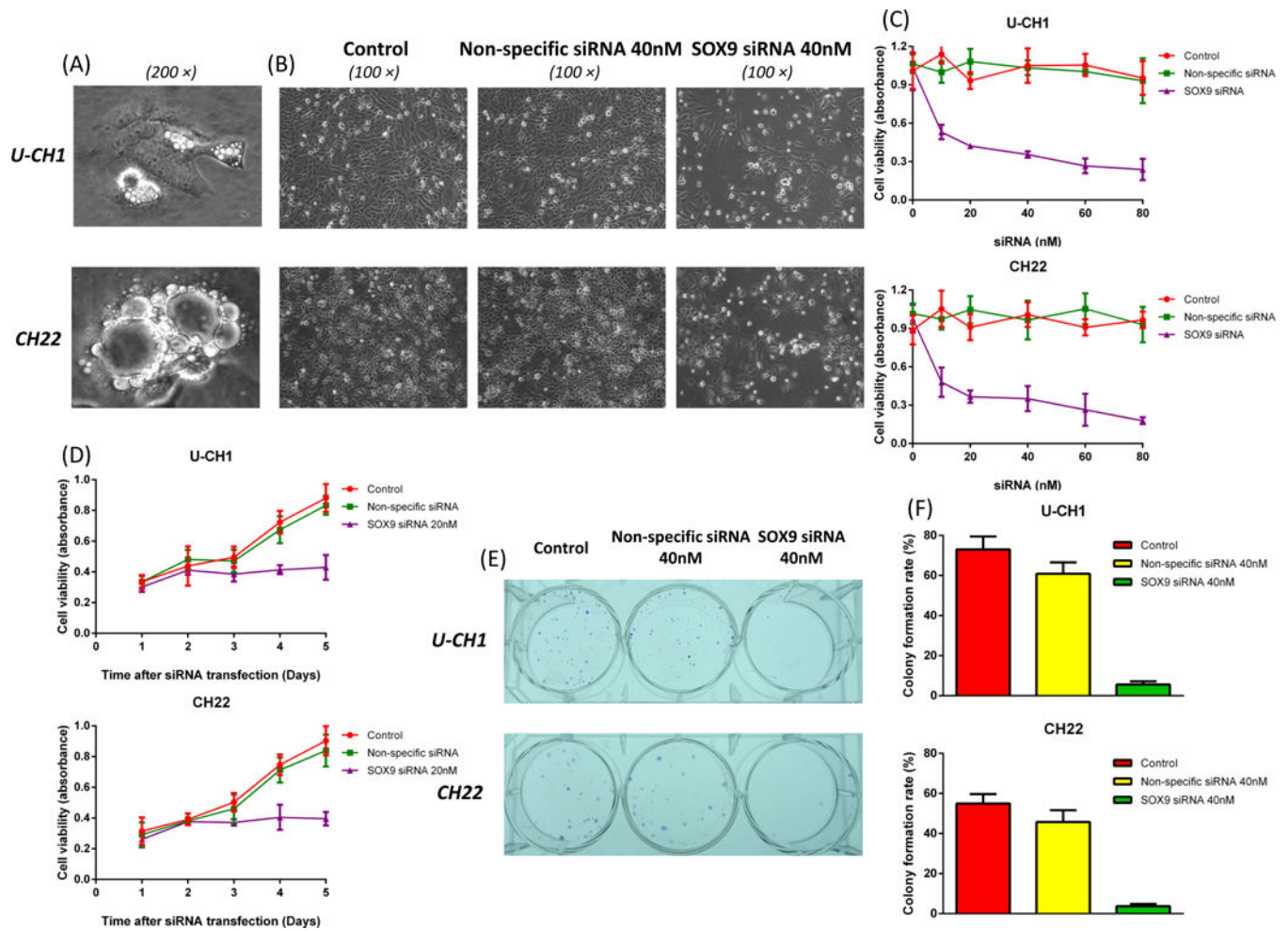


Figure 2.

Inhibition of SOX9 by RNAi blocks proliferation in chordoma cell lines. (A) Light microscopy of U-CH1 and CH22 cells reveals the classical appearance of chordoma, which is characterized by a round nucleus with clear cytoplasmic vacuoles. Original magnification: 200 \times . (B) Representative images of chordoma cells after treatment with non-specific siRNA or SOX9 siRNA. Original magnification: 100 \times . (C) The MTT assay revealed dose-dependent inhibition of cell proliferation after SOX9 siRNA treatment was applied to U-CH1 and CH22 cell lines. (D) The MTT assay revealed time-dependent inhibition of cell proliferation after SOX9 siRNA treatment was applied to U-CH1 and CH22 cell lines. (E) Representative images of chordoma cell colony formation after treatment with non-specific siRNA or SOX9 siRNA. (F) The clonogenic assay revealed a reduced rate of cell colony formation after the treatment of non-specific siRNA or SOX9 siRNA in U-CH1 and CH22 cells.

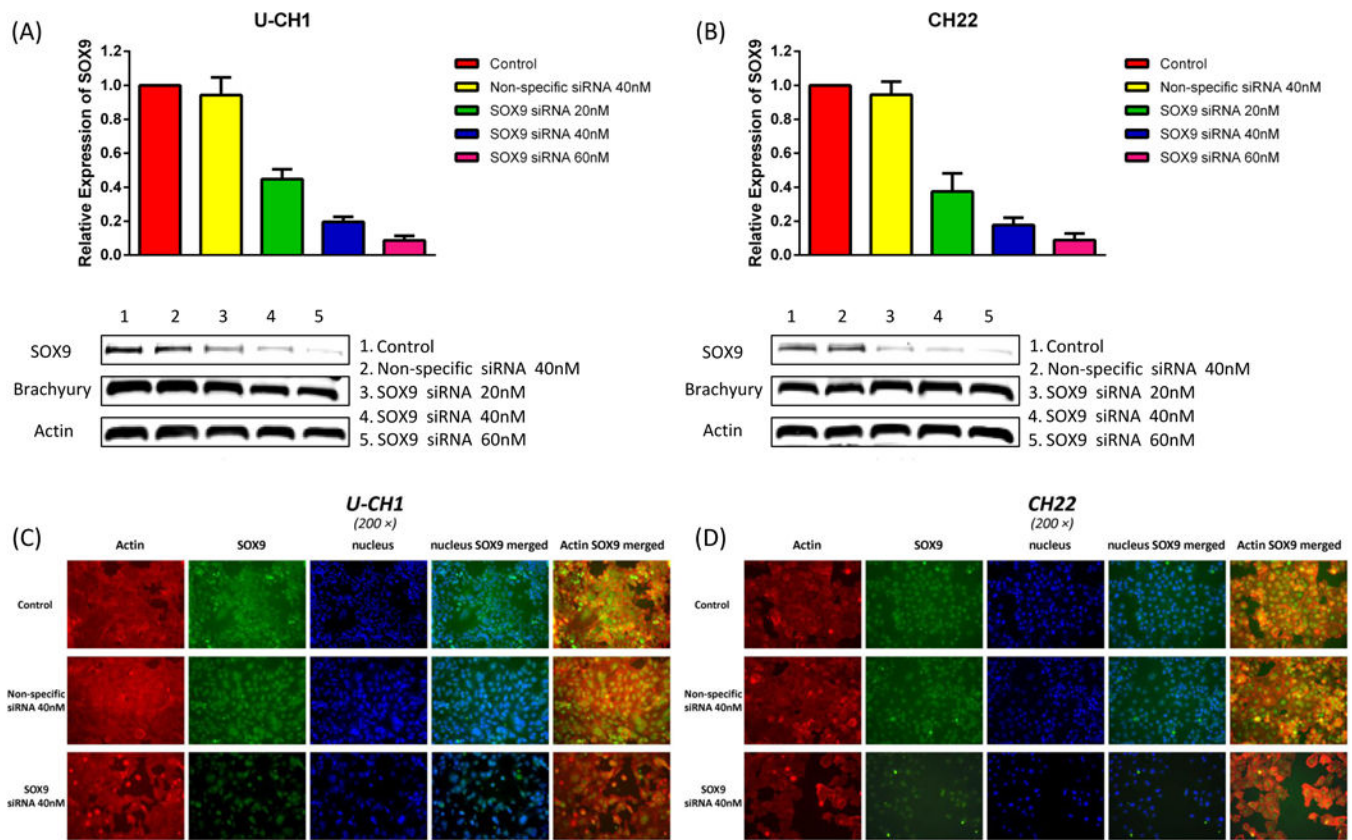


Figure 3. SOX9 and brachyury protein expression alteration after treatment of chordoma cell lines with non-specific siRNA or SOX9 siRNA. (A and B) Western blot and semi-quantitative analysis done after the SOX9 siRNA transfection in U-CH1 and CH22 cell lines reveal a knockdown in SOX9 expression and no alteration of brachyury expression. (C and D) Confirmation of the knockdown of SOX9 protein expression after SOX9 siRNA transfection in U-CH1 and CH22 cell lines as determined by immunofluorescence.

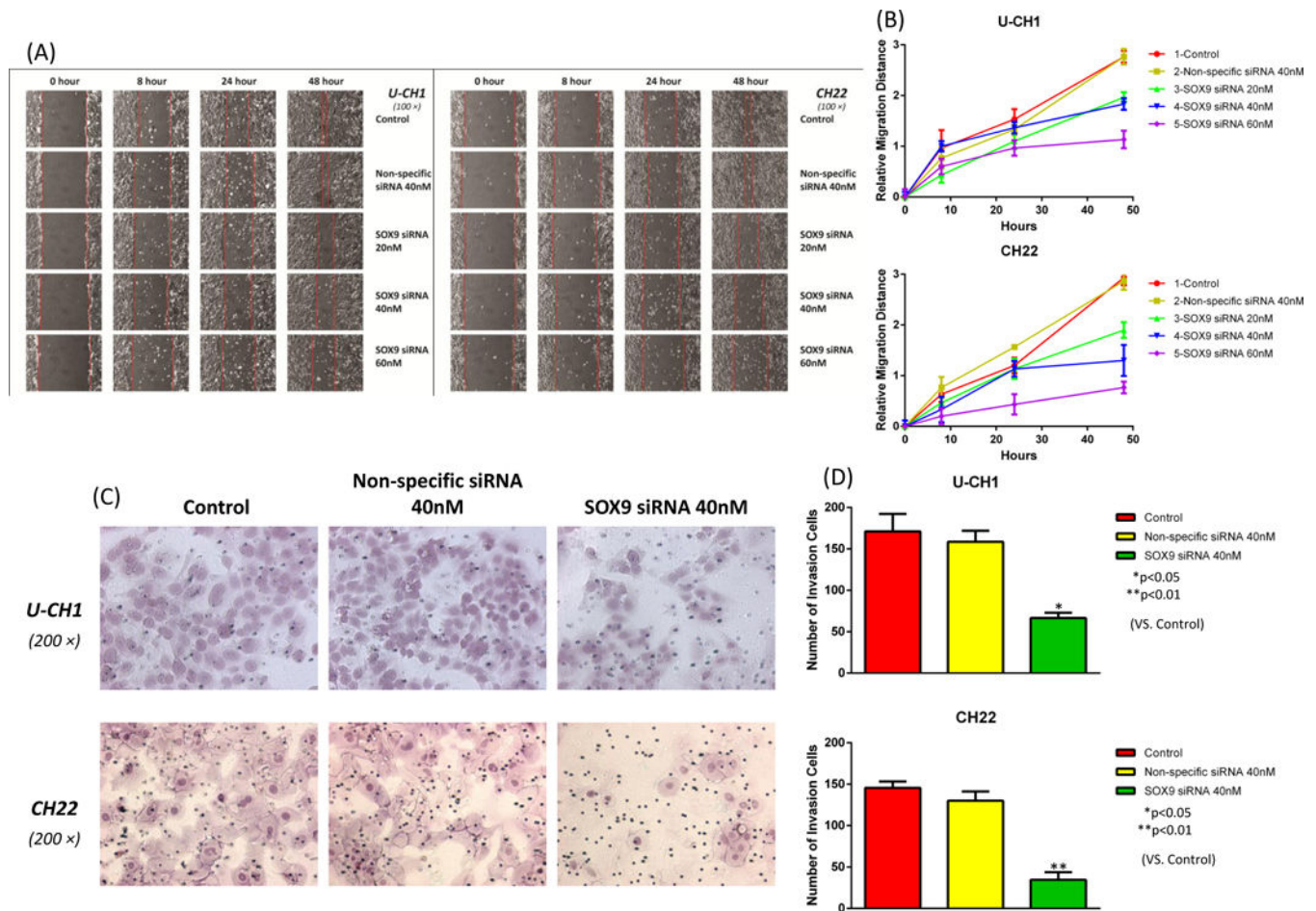
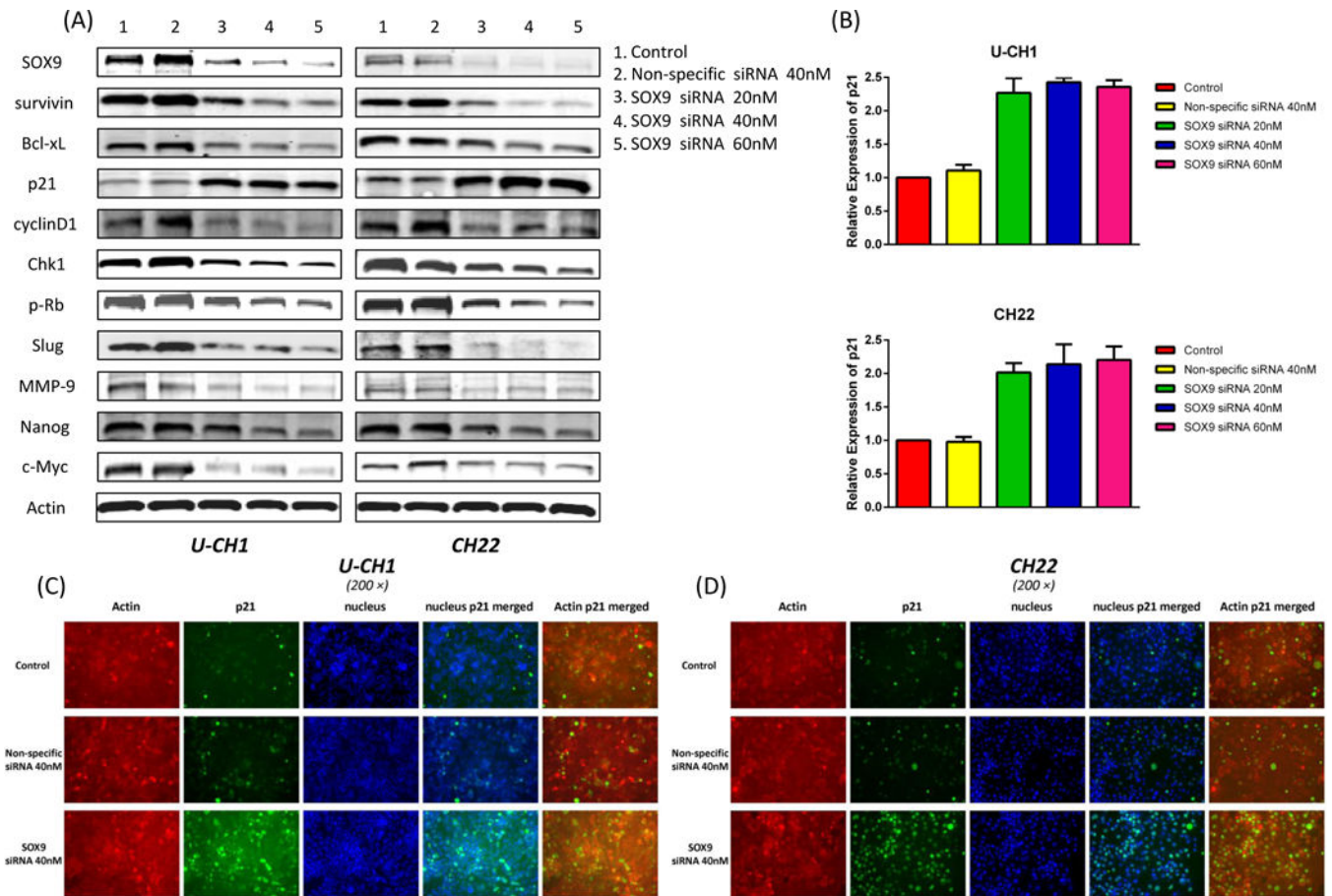


Figure 4. Inhibition of SOX9 by RNAi impairs motility in chordoma cell lines. (A) Representative migration images of U-CH1 and CH22 cell lines at different time points (0, 8, 24, and 48 hours) when treated with different concentrations of SOX9 siRNA and non-specific siRNA. Original magnification: 100 \times . (B) Relative migration distance of U-CH1 and CH22 at different time points (0, 8, 24, and 48 hours) when treated with different concentrations of SOX9 siRNA and non-specific siRNA. (C) Representative invasion images. Original magnification: 200 \times . (D) The number of invasive U-CH1 and CH22 cells in the Matrigel after treatment with SOX9 siRNA and non-specific siRNA for 48 hours.

**Figure 5.**

Inhibition of SOX9 by siRNA transfection results in related protein alterations in chordoma cell lines. (A) Representative Western blot analysis done after the transfection of SOX9 siRNA and non-specific siRNA in U-CH1 and CH22 cell lines revealed proteins involved in apoptosis, cell cycle, migration, and stem cell alterations. (B) Upregulation of p21 expression after SOX9 siRNA transfection in U-CH1 and CH22 cell lines as determined by semi-quantitative analysis. (C and D) Confirmation of the upregulation of p21 protein expression after SOX9 siRNA transfection in U-CH1 and CH22 cell lines as determined by immunofluorescence.

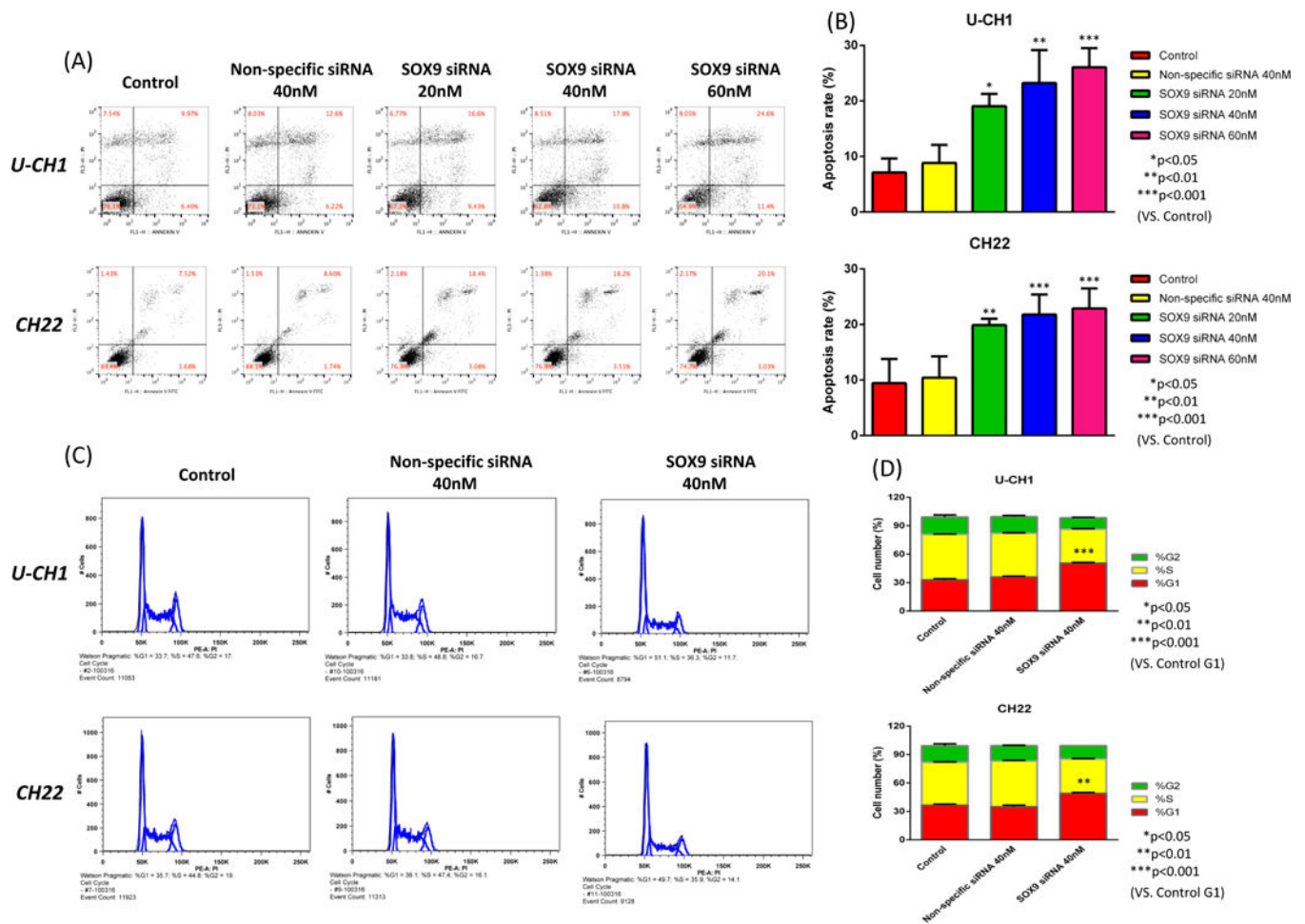


Figure 6. Inhibition of SOX9 by siRNA transfection induces cell apoptosis and cell cycle arrest in chordoma cell lines. (A) Representative results of flow cytometric analysis of cell apoptosis in U-CH1 and CH22 cell lines, incubated with different concentrations of SOX9 siRNA and non-specific siRNA. (B) Analysis of the rate of apoptosis in U-CH1 and CH22 cell lines treated with different concentrations of SOX9 siRNA and non-specific siRNA. (C) Representative results of flow cytometric analysis of cell cycle in U-CH1 and CH22 cell lines that were incubated with SOX9 siRNA and non-specific siRNA. (D) Alterations in cell cycle phases and their distributions amongst U-CH1 and CH22 cells treated with SOX9 siRNA and non-specific siRNA.